environmental microbiology

Environmental Microbiology (2016) **18**(6), 1863–1874 doi:10.1111/1462-2920.13058

Transient dynamics of competitive exclusion in microbial communities

Stilianos Louca[1]* and Michael Doebeli[2,3]
[1]*Biodiversity Research Centre, University of British Columbia, Vancouver, BC V6T 1Z4, Canada.*
[2]*Department of Zoology, University of British Columbia, Vancouver, BC V6T 1Z4, Canada.*
[3]*Department of Mathematics, University of British Columbia, Vancouver, BC V6T 1Z2, Canada.*

Summary

Microbial metabolism drives our planet's biogeochemistry and plays a central role in industrial processes. Molecular profiling in bioreactors has revealed that microbial community composition can be highly variable while maintaining constant functional performance. Furthermore, following perturbation bioreactor performance typically recovers rapidly, while community composition slowly returns to its original state. Despite its practical relevance, we still lack an understanding of the mechanisms causing the discrepancy between functional and compositional stability of microbial communities. Using a mathematical model for microbial competition, as well as simulations of a model for a nitrifying bioreactor, we explain these observations on grounds of slow non-equilibrium dynamics eventually leading to competitive exclusion. In the presence of several competing strains, metabolic niches are rapidly occupied by opportunistic populations, while subsequent species turnover and the eventual dominance of top competitors proceeds at a much slower rate. Hence, functional redundancy causes a separation of the time scales characterizing the functional and compositional stabilization of microbial communities. This effect becomes stronger with increasing richness because greater similarities between top competitors lead to longer transient population dynamics.

Introduction

Microbial metabolism drives the biochemistry of virtually all ecosystems and plays a central role in industrial processes such as biofuel production and wastewater treatment (Falkowski *et al*., 2008; Antolli and Liu, 2012). Thus, understanding the mechanisms that shape the dynamics and metabolic performance of microbial communities is of great practical importance. Experiments with bioreactors have shown that bioreactor performance can be constant despite highly variable microbial communities (Wang *et al*., 2011). For example, following functional stabilization, methanogenic or nitrifying bioreactors can exhibit species turnover for several more years (Fernández *et al*., 1999; Wittebolle *et al*., 2008). In some cases non-convergent community trajectories have been reproduced across replicated experiments, suggesting that the underlying processes are deterministic (Ayarza *et al*., 2010; Vanwonterghem *et al*., 2014). Even when communities converge to a steady composition, recovery of community composition following perturbation can take several months. This is in contrast to metabolic throughput, which recovers within a few days (Sundh *et al*., 2003; Gentile *et al*., 2006). Fluctuations and the rate of stabilization of microbial communities are thus multifaceted properties that depend greatly on whether the focus is on metabolic function or taxonomic composition. An improved understanding of these properties in microbial communities is crucial for optimizing microbially driven industrial processes and interpreting the response of ecosystems to anthropogenic perturbations.

It has been hypothesized that functional redundancy and non-equilibrium population dynamics within each metabolic compartment could promote fast stabilization of performance with slow convergence of community composition (Briones and Raskin, 2003). Here we show that temporary population dynamics leading to an eventually steady community composition via competitive exclusion can indeed last much longer than the time required for the stabilization of overall metabolic performance. We first formalize our reasoning using a microbial community model, in which multiple strains compete for a common resource. The model illustrates in a simple way how taxonomic community composition can vary almost independently of the community's metabolic performance. We then construct a more realistic model of a nitrifying bioreactor and use simulations to demonstrate the validity of our arguments and their consistency with previous experimental observations.

Received 30 June, 2015; accepted 15 September, 2015. *For correspondence. E-mail louca@zoology.ubc.ca; Tel. +1 604 822 1921; Fax +1 604 822 0957.

Results and discussion

Competition for a common resource

Microbial community richness can be disproportionally high compared with the metabolic complexity of bioreactors, whereas the coexistence of metabolically similar organisms has been contrasted to the competitive exclusion principle (Hardin, 1960; Fernández *et al*., 1999; Fernandez *et al*., 2000; Wittebolle *et al*., 2009). In the case of a single limiting resource, Tilman's (1982) competition theory predicts that at equilibrium the only persisting competitor will be the one that can survive at the lowest resource concentration. However ecosystems can be subject to long transient dynamics, i.e. temporary population dynamics far from equilibrium, and convergence to equilibrium might occur at much longer time scales than assumed (Hastings, 2004). For example, slow species turnover has been suggested to be responsible for the perplexingly high diversity seen in many microbial systems (Chesson, 2000) and, as we show here, can explain the discrepancy between functional and taxonomic stability in bioreactors.

To formalize our argument, we use a model for multiple populations competing for the same limiting resource. We focus on the transient dynamics eventually leading to steady state, where resource input is balanced by microbial consumption. The cell density of strain *i*, denoted by N_i, as well as the resource concentration, denoted by R, are described by the following differential equations:

$$\frac{dN_i}{dt} = N_i\left[\beta_i \Phi_i(R) - \lambda_i\right], \tag{1}$$

$$\frac{dR}{dt} = f_o - \sum_i N_i \Phi_i(R). \tag{2}$$

Here, f_o is the constant resource supply rate, λ_i is the decay rate of strain *i* in the absence of growth, $\Phi_i(R)$ is the rate at which cells take up the resource as a function of R, and β_i is a biomass yield factor. We assume that $\Phi_i(R)$ increases with R. For example, $\Phi_i(R)$ could be a Monod function that increases linearly with R at low concentrations but saturates at high concentrations, an assumption often made in geobiological and bioengineering models (Jin *et al*., 2013). The last term in Eq. 2 is a sum over all strains accounting for resource depletion by microbial metabolism.

The growth rate of strain *i* is positive whenever R is greater than the threshold concentration, R_i^o, defined by $\Phi_i(R_i^o) = \lambda_i/\beta_i$. In general, the equilibrium of Eqs. 1 and 2 is characterized by the extinction of all but one strain, namely the strain with the lowest survival threshold R_i^o. To elucidate the transient dynamics preceding this competitive exclusion, we consider the total cell density $N = \sum_i N_i$ and the relative cell densities $\eta_i = N_i/N$. Using the community-average growth kinetics (denoted $\overline{\Phi}$, $\overline{\beta\Phi}$ and $\overline{\lambda}$), one can derive the dynamics

$$\frac{d\eta_i}{dt} = \varepsilon_i \cdot \eta_i\left(\overline{\beta\Phi} - \overline{\lambda}\right) \tag{3}$$

for the relative cell densities,

$$\frac{dN}{dt} = N\left(\overline{\beta\Phi} - \overline{\lambda}\right) \tag{4}$$

for the total cell density N, and

$$\frac{dR}{dt} = f_o - N\overline{\Phi} \tag{5}$$

for the resource concentration R (details found in Supporting Information). Here, the ε_i account for deviations of strain *i* growth kinetics from the community average. For example, if N is growing and ε_i is positive, then strain *i* grows faster than average and thus increases in relative abundance.

As the resource is depleted, weaker competitors decay and the average growth kinetics are determined by a few remaining competitors of similar efficiency, for which the deviations ε_i from the average become very small ($\varepsilon_i << 1$). Hence, while the dynamics of N and R are determined by the community-average growth kinetics (Eqs. 4 and 5), the relative cell densities are slowed down by the factors ε_i. This means that while metabolic niches are quickly filled, establishing a high rate of resource uptake, some of the competing populations can coexist during prolonged transition periods until eventual competitive exclusion. In agreement with these predictions, Gentile and colleagues (2006) report a quick functional stabilization and long transient periods in community composition following mechanical shock, and Vanwonterghem and colleagues (2014) report a gradually decreasing richness in anaerobic digesters over the course of several months following inoculation.

The probability of similar strains being present in a random inoculum, or a microbial community in general, increases with the number of strains. In particular, the expected dissimilarity between top competitors decreases with increasing community richness. The underlying assumption is that growth kinetic parameters are bound within some natural finite range. Hence, one should expect longer transient dynamics of competitive exclusion and slower convergence to a steady community composition at higher inoculum richness.

It has been previously hypothesized that as richness increases, the variability of ecosystem functions decreases, whereas the variability of individual populations increases (Tilman, 1996; Lehman and Tilman, 2000; Loreau *et al*., 2001). The proposed mechanisms typically involve stochastic fluctuations of independent populations, so that the total community biomass and functional

performance become more stable when more populations contribute to them. This statistical inevitability (Doak *et al*., 1998), which has been criticized on grounds of interspecific interactions (Tilman *et al*., 1998), differs fundamentally from the deterministic mechanisms explored here. Namely, competition between strains leads to a slow decay of weaker competitors, which is compensated by the growth of other populations that stabilize overall functional performance.

Bioreactors as model systems

The above competition model explains how populations occupying a common metabolic niche can, in principle, undergo long transient periods of coexistence. The actual duration and nature of these transients depend on the similarity between competing strains, as well as their typical intrinsic growth kinetics. To test the relevance of our predictions to realistic microbial communities, we examined a separate numerical model for a nitrifying bioreactor (Wittebolle *et al*., 2008). Apart from their practical relevance to industrial processes such as sewage treatment and biofuel production (Antolli and Liu, 2012), bioreactors are also ideal model systems for understanding microbial ecology and processes shaping microbial community structure (Fernandez *et al*., 2000; Graham *et al*., 2007; Vanwonterghem *et al*., 2014). The bioreactor considered here is a flow-through chemostat continuously fed with ammonium (NH_4^+), which is aerobically oxidized to nitrate (NO_3^-) in a two-step process. Oxidation occurs in a microbial community that consists of chemoautotrophic ammonium-oxidizing bacteria (AOB), which transform ammonium to nitrite (NO_2^-), and chemoautotrophic nitrite-oxidizing bacteria (NOB), which transform nitrite to nitrate. Nitrate is exported from the bioreactor as part of a continuous outflow through a filter membrane that retains cells within the bioreactor. The substrate feed rate and the hydraulic dilution rate are kept constant and in line with previous bioreactor experiments (Wittebolle *et al*., 2008), allowing the establishment of a steady metabolic throughput following an initial start-up period.

The bioreactor's microbial community is modelled using differential equations for the cell population densities and the ambient ammonium, nitrite and nitrate concentrations. These metabolites are subject to microbial production and depletion, as well as physical addition and removal from the bioreactor. The metabolic activity of individual cells is determined using flux balance analysis (FBA), a widely used framework in cell-metabolic modelling (Orth *et al*., 2010). In FBA, the chemical state of cells is assumed to be steady, leading to stoichiometric constraints that need to be satisfied for any particular combination of intracellular reaction rates. These rates are assumed to be regulated by the cell in such a way that some objective function, commonly associated with biomass production, is maximized subject to additional constraints on substrate uptake rates (Feist and Palsson, 2010). In our case, the optimized biosynthesis rate is translated to a growth rate by dividing by the cell mass. Ammonium and nitrite uptake rates are limited by substrate concentrations in a Monod-like fashion, thus constraining the achievable growth rates depending on the bioreactor's chemical state (Mahadevan *et al*., 2002; Harcombe *et al*., 2014).

The assumption of cells maximizing biosynthesis, subject to environmental and physiological constraints, is rooted in the idea that evolution has shaped regulatory mechanisms to induce maximum growth whenever possible (Burgard and Maranas, 2003; Harcombe *et al*., 2013). This assumption is less valid for genetically engineered organisms or those exposed to environments that are radically different from the environments that shaped their evolution, and other objectives such as ATP production or metabolic efficiency have been proposed (Segrè *et al*., 2002; Gianchandani *et al*., 2008). Biosynthesis has been experimentally verified as an objective for, among others, *Saccharomyces cerevisiae*, *Escherichia coli* and *Nitrosomonas europaea* (Duarte *et al*., 2004; Feist and Palsson, 2010; Perez-Garcia *et al*., 2014). Despite its limitations, FBA with maximization of growth has greatly contributed to the understanding of several single-cell metabolic networks as well as metabolic interactions between cells (Klitgord and Segrè, 2010; Orth *et al*., 2010; Freilich *et al*., 2011; Chiu *et al*., 2014). One advantage of FBA models over full biochemical cell models is their independence of intracellular kinetics and gene regulation, which limits the number of required parameters to stoichiometric coefficients and uptake kinetics. Recent work has shown that FBA-based models with maximization of growth can accurately predict microbial community dynamics (Meadows *et al*., 2010; Chiu *et al*., 2014; Harcombe *et al*., 2014; Louca and Doebeli, 2015).

Our bioreactor model comprises multiple AOB and NOB strains, which are constructed by randomly choosing several cell parameters around those of two template AOB and NOB models. The AOB and NOB templates were calibrated and validated beforehand using data from previous bioreactor experiments (Fig. 1; see Experimental Procedures for details). Because metabolites can be depleted or produced by several cells, the environmental metabolite pool mediates the metabolic interactions between cells (Schink and Stams, 2006). For example, AOB deplete ammonium from their environment, rendering it a limiting resource that mediates competition between AOB strains. The excretion of nitrite as a by-product, in turn, enables the growth of nitrite-limited NOB. The metabolic optimization of individual cells striving for maximal growth, while modifying their environment,

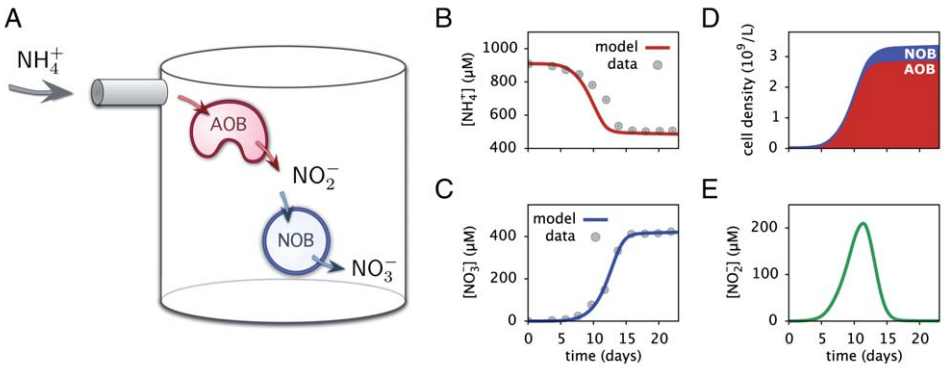

Fig. 1. Calibration and validation of the template AOB and NOB cell models using data from experiments with a nitrifying batch-fed bioreactor (A). Ammonium (NH_4^+) was added at the beginning of the experiment, and was sequentially oxidized to nitrite (NO_2^-) and nitrate (NO_3^-) by a growing nitrifier community. (B) and (C): Ammonium (B) and nitrate (C) concentration time series data (dots), compared with the calibrated model (continuous lines). (D): AOB and NOB cell densities over time, as predicted by the model. (E): Nitrite concentration over time, as predicted by the model. Experimental data from de Boer and Laanbroek (1989). Note that while the template cell models were calibrated using batch-bioreactor experiments, for our subsequent analysis we consider continuously fed flow-through bioreactors because these can support metabolically active microbial communities at steady state.

thus leads to non-trivial community dynamics that can include cooperation, competition and extinction.

Bioreactor community dynamics

Following inoculation of the bioreactor, two phases can generally be distinguished (Fig. 2): Initially, the concentration of inflowing ammonium increases until AOB populations have grown to sufficient densities to balance ammonium supply by ammonium consumption. The accumulation of nitrite as an AOB waste product, in turn, triggers the growth of NOB populations until nitrite production is eventually balanced by nitrite consumption. This initial startup phase is dominated by fast-growing opportunists

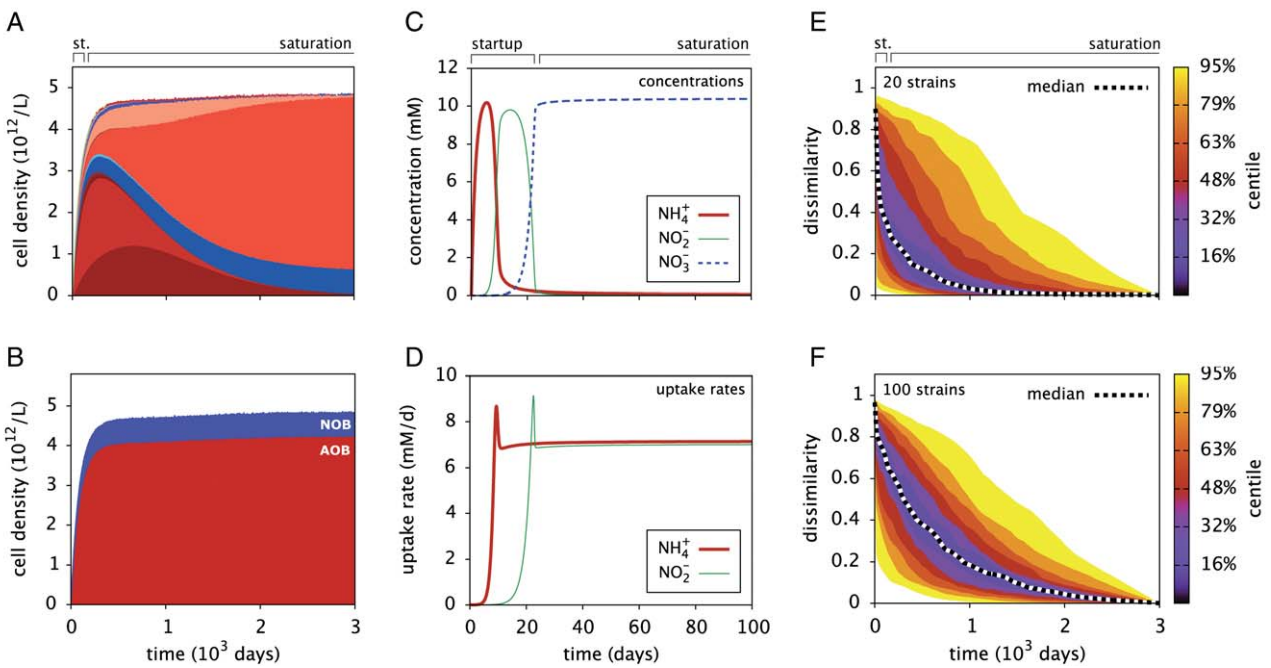

Fig. 2. (A) Simulated cell densities over time in the ammonium-fed nitrifying membrane bioreactor, inoculated with 100 random strains (AOB in variations of red, NOB in variations of blue). (B) Corresponding total cell densities per functional group (AOB or NOB). (C) Corresponding ammonium (NH_4^+), nitrite (NO_2^-) and nitrate (NO_3^-) concentrations. (D) Corresponding community-wide ammonium and nitrite uptake rates. (E, F): Bray–Curtis dissimilarity of the community to the long-term steady state, following inoculation with 20 (E) or 100 (F) random strains. Shown as a probability distribution over 100 random simulations (colours correspond to centiles). Notice the faster rate of convergence to steady state (i.e. resilience) in (E) compared to (F). The two intervals on the top of figures (A, C, E) indicate rough start-up and saturation phases respectively.

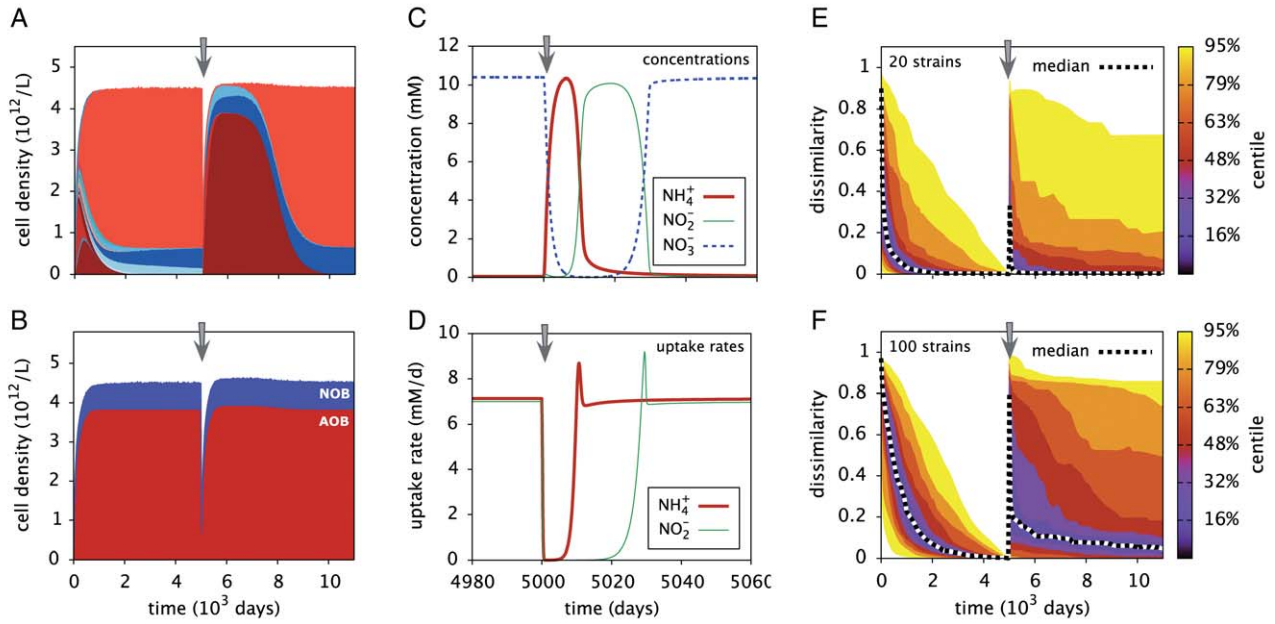

Fig. 3. (A) Simulated cell densities over time in the ammonium-fed nitrifying membrane bioreactor, inoculated with 100 random strains (AOB in variations of red, NOB in variations of blue). A strong perturbation during day 5000 (grey arrow) causes a temporary collapse of the microbial community. (B) Corresponding total cell densities per functional group (AOB or NOB). (C) Corresponding ammonium (NH_4^+), nitrite (NO_2^-) and nitrate (NO_3^-) concentrations, at times near the perturbation. (D) Corresponding community-wide ammonium and nitrite uptake rates, at times near the perturbation. (E, F) Bray–Curtis dissimilarity of the community to the state shortly prior to the perturbation, in bioreactors inoculated with 20 (E) or 100 (F) random strains. Shown as a probability distribution over 100 random simulations (colours correspond to centiles). Notice the greater resistance to perturbation and greater resilience in (E) compared to (F).

that benefit from an excess of substrates and little competition. The duration of this phase is mainly determined by the hydraulic renewal rate, ammonium supply rate and bacterial growth rates, and the duration predicted by our model (roughly 3 weeks) is in line with typical nitrifying bioreactor experiments (Dumont *et al*., 2009; Martens-Habbena *et al*., 2009).

As ammonium and nitrite consumption increase, their concentrations decrease to near or below the survival thresholds for an increasing number of strains (Fig. 2C). This second saturation phase is characterized by low and relatively stable substrate concentrations, stagnation of growth, a gradual extinction of less competitive strains and a long coexistence of similar top competitors (Fig. 2A). The microbial community slowly converges to a stable composition of decreased diversity in which each metabolic niche is occupied by a single strain, with transient periods occasionally lasting up to several thousands of days. A gradual decrease in diversity is expected under the competitive exclusion principle of equilibrium ecology (Hardin, 1960) and is consistent with similar observations in previous bioreactor experiments (Vanwonterghem *et al*., 2014). On the other hand, the total cell densities of metabolically similar strains (e.g. AOB) stabilize much faster and only vary weakly during the saturation phase (Fig. 2B). Hence, each of the two available metabolic niches is rapidly filled by several competing and temporarily coexisting strains, which are only slowly replaced by the top competitor.

These results show how transient dynamics of competitive exclusion can lead to a separation of time scales characterizing functional and compositional stabilization of communities. This separation of time scales is also expected to be reflected in the community's response to perturbations. Perturbations such as mechanical biofilm removal (Gentile *et al*., 2006) or nutrient shocks (Sundh *et al*., 2003) can alter the relative abundances of individual clades or lead to a temporary collapse of the community. Such a collapse would initiate a race for the (re-)occupation of metabolic niches and a subsequent saturation phase, analogous to the dynamics following inoculation. For example, Gentile and colleagues (2006) observed that after the shearing of biofilms inside a fluidized bed reactor community composition recovered much slower, i.e. it had lower resilience (Shade *et al*., 2012), than the bioreactor's performance.

Simulations of the bioreactor model including a strong pulse perturbation, applied simultaneously to the entire community, reproduced these observations (Fig. 3). The modelled perturbation corresponds to an increased mortality for 1 day, with a strength chosen randomly for each strain and resulting in a temporary collapse of the community by several orders of magnitude. Consistent with experimental observations, the bioreactor's performance

quickly recovers within a few days to weeks (Fig. 3C and D), whereas the community's recovery to its original composition typically takes several months to years (Fig. 3A,E,F). Metabolic niches are reoccupied rapidly and concurrently with the bioreactor's functional stabilization (Fig. 3B); however, metabolic niches can be temporarily shared by several coexisting strains. Non-equilibrium processes, particularly following perturbation, are frequently thought to maintain high diversity, for example in rain forests (Connell, 1978) or phytoplankton (Sommer, 1984). Furthermore, a meta-analysis by Shade and colleagues (2012) found more studies reporting the recovery of microbial community function than composition, following pulse perturbation.

As predicted above by our competition model, the discrepancy between functional and taxonomic stability should be stronger for communities with high richness because the likelihood of two similar top competitors increases, thus delaying competitive exclusion. Simulations of bioreactors inoculated with different numbers of random strains verify this prediction. For example, the time until compositional convergence following inoculation, i.e. reaching a 90% Bray–Curtis similarity to the steady state (Legendre and Legendre, 1998), ranges from roughly 600 days for 20 strains to 1300 days for 100 strains (median values, Fig. 2E and F). Moreover, richer communities are expected to be more prone to temporary changes in composition during perturbation because of a greater reservoir of opportunistic strains that could temporarily invade (Wittebolle *et al*., 2008). This is reflected in our simulations, where a greater number of strains correlates with a stronger change in community composition following the pulse perturbation (Fig. 3E and F). The insensitivity to disturbance is known in ecology as resistance and is, together with resilience, a common measure of community stability (Shade *et al*., 2012). Our work suggests that microbial communities with higher functional redundancy have lower resilience and lower resistance to pulse perturbation in terms of taxonomic composition.

Variable does not mean unstable

Previous bioreactor experiments have revealed variable community composition despite stable bioreactor performance over hundreds of days following inoculation (Fernández *et al*., 1999; Zumstein *et al*., 2000; Wittebolle *et al*., 2008; Vanwonterghem *et al*., 2014), whereas others have reported convergence to steady compositions within a few months (Xing *et al*., 1997; Gentile *et al*., 2006; McGuinness *et al*., 2006). Fluctuating community compositions are often interpreted as unstable, non-convergent or even chaotic. However, the observed dynamics may be mere transients of slowly converging communities. Typical richness in bioreactors can range from hundreds to thousands of operational taxonomic units (OTUs, a species analogue based on rDNA similarity) (Stackebrandt *et al*., 2002; Kim *et al*., 2013; Vanwonterghem *et al*., 2014). As shown here, at these richness scales transient dynamics of competitive exclusion can last several years. Much longer operation times might thus be needed to actually observe an eventual community convergence in typical bioreactors. However, at these time scales other destabilizing processes, such as the invasion of new strains introduced by contamination, could prevent community convergence.

Model limitations

The simple models considered in this paper focus on generic ingredients of microbial ecosystems, namely substrate-limited growth and competition, stoichiometric constraints on coexisting pathways, as well as physical substrate repletion and waste removal (e.g. in continuous-flow bioreactors). In particular, we have assumed that microbial growth increases with increasing substrate concentrations, thus ignoring the possibility of substrate inhibition. For example, substrate inhibition can occur during nitrification by excess ammonia and nitrous acid (Anthonisen *et al*., 1976), resulting in reduced bioreactor performance (Sheintuch *et al*., 1995). Similarly, growth may also be subject to product inhibition, e.g. when the partial pressure of accumulating waste products renders a pathway unfavourable (Kaspar and Wuhrmann, 1977). Accurately modelling specific industrial setups may thus require a consideration of more complicated kinetics, e.g. including substrate and product inhibition. Our main point is that long transient dynamics can emerge even in the simple cases considered here, acknowledging that more complex communities are likely subject to further destabilizing mechanisms (see below).

Alternative destabilizing factors

Transient dynamics of competitive exclusion provide a simple explanation for the discrepancy between functional and taxonomic stability of microbial communities, and our simulations underline the relevance of these processes at least to typical bioreactor setups. However, other mechanisms likely contribute to a long-term variability of community composition. For example, time lags associated with the degradation of organic matter, such as cellulose hydrolysis in anaerobic digesters (Vanwonterghem *et al*., 2014), can result in slow changes of the metabolic landscape and optimal electron flow, in turn driving adaptive changes in community composition (Fernández *et al*., 1999). More complicated non-sequential pathways, ubiquitous in organic carbon catabolism, could also lead to positive feedback loops that further destabilize community dynamics. Furthermore, in contrast to well-controlled

bioreactors, many natural ecosystems are subject to intense environmental variation that can drive adaptation and succession in microbial communities. For example, annual deep-water renewal in a seasonally anoxic fjord has been shown to cause significant changes in microbial community structure (Zaikova *et al*., 2010).

We emphasize that mechanisms that destabilize community composition need not necessarily destabilize community function. For example, in open systems such as wastewater treatment plants (Wang *et al*., 2011) occasional invasion by novel competitors could drive species turnover without significantly affecting ecosystem functioning; however, this scenario is unlikely in bioreactors with a sterile feed (Vanwonterghem *et al*., 2014). Similarly, repeated adaptation of bacteriophages to dominant hosts ('killing the winner' dynamics) has been shown to sustain bacterial diversity and drive continuous species turnover (Thingstad, 2000; Shapiro and Kushmaro, 2011). Collapsing populations could be replaced by less susceptible but functionally similar populations that ensure the overall stability of biochemical fluxes.

Reciprocally, negative feedback mechanisms stabilizing biochemical fluxes may only weakly affect community composition. For example, substrate built-up can promote the growth of functional groups benefiting from the underutilized resource, in turn counteracting the processes causing substrate built-up. This stabilizing mechanism, perhaps comparable with La Châtelier's principle of an 'opposing force' (Schneider, 2004), a priori acts on functional groups rather than taxonomy.

Towards a pathway-centric microbial ecology

Environmental rDNA marker gene profiling has become a standard approach in microbial ecology for describing community composition in terms of OTUs (Wittebolle *et al*., 2008; Gilbert *et al*., 2010). However, single prokaryotic OTUs can comprise several distinct ecotypes (Welch *et al*., 2002; Kashtan *et al*., 2014) and, reciprocally, ecologically important pathways such as nitrogen fixation can exhibit non-monophyletic distributions across distant clades (Raymond *et al*., 2004; Frigaard *et al*., 2006). In fact, environmental conditions and ecological function often show a stronger correlation to particular metabolic pathways or even individual genes, than to the presence or absence of particular clades (Ofiţeru *et al*., 2010; Burke *et al*., 2011; Raes *et al*., 2011). Consistent with this, as we have shown here, compositional stability can be independent from functional stability while key genes (for example ammonia monooxygenase, present in AOB) remain synchronized with the community's performance. Hence, prokaryotic OTUs should be questioned as an ecologically relevant unit altogether (Gevers *et al*., 2005; Ward *et al*., 2007; Doolittle and Zhaxybayeva, 2010). Microbial ecology and biogeography might be best understood using function-centric theories in which individual genes, operons or pathways are considered as basic reproductive and functional units, particularly under conditions where metabolic functions define the microbial niche space (Dumont *et al*., 2009; Reed *et al*., 2014). Accordingly, metagenomic, metatranscriptomic and metaproteomic profiling would be more suitable than marker genes for monitoring or predicting fluctuations of community function (Ward *et al*., 2007; Doolittle and Zhaxybayeva, 2010; Hawley *et al*., 2014).

Conclusions

Convergence of microbial community composition is a gradual process that can last much longer than typical bioreactor experiments and environmental surveys. Transient dynamics of competitive exclusion explain why microbial communities can remain variable long after inoculation or perturbation, while exhibiting high functional stability. The correct interpretation of observed community dynamics in bioreactors and natural ecosystems thus requires a proper consideration of the involved time scales. Previous work has highlighted the general mismatch between the duration of typical experiments and the time scales assumed by conventional steady-state ecological theories (Hastings, 2004), and our work demonstrates some of the implications of this mismatch. Fluctuations in natural and less controlled microbial communities likely result from several destabilizing processes; however, the effects of these processes could be augmented by transient dynamics of competitive exclusion.

Furthermore, less resilient and more flexible communities need not imply a compromised functional stability, and previous experiments have indeed indicated a positive correlation between flexible community structure and stable performance (Fernandez *et al*., 2000). Several competing strains can rapidly and concurrently fill a metabolic niche when opportunities arise, while slowly replacing each other and maintaining constant performance during saturation. The time required for convergence or recovery of community composition correlates positively with functional redundancy because more competitors are likely to have similar efficiencies under substrate limitation.

The extreme case in which each functional group consists of equal competitors is comparable with the so-called emergent group theory in ecology, according to which assembly within each group is subject to neutral dynamics (Hubbell, 2005; Hérault, 2007). In that limit, transient periods of competitive exclusion can be extremely long, whereas community composition appears dissociated from environmental conditions and driven by purely stochastic factors. Although exact neutrality is an extreme idealization, some natural communities may

indeed include functional groups consisting of almost-equal competitors. For example, previous work on a wastewater treatment plant found that fluctuations within the group of ammonia-oxidizing bacteria, as well as within the heterotrophic community, were predominantly explained by neutral processes rather than environmental factors (Ofiţeru *et al*., 2010). Similarly, a global study of desert microbial communities by Caruso and colleagues (2011) found that climatic effects were detectable at the whole community level, but became undetectable when restricted to variations within the photosynthetic or heterotrophic groups. Frossard and colleagues (2012) found that spatiotemporal variations of microbial community structure in stream catchments were best described by a neutral assembly model, whereas potential activities of several carbon-, nitrogen- and phosphorus-acquiring enzymes showed clear seasonal patterns. This discrepancy between potential enzyme activities and the composition of their host communities indicates high functional redundancy and a decoupling between community function and taxonomy. Similarly, Yin and colleagues (2000) showed significant functional redundancy in soil microbial communities by measuring population responses to enrichment with individual carbon sources. However, it is unclear whether all detected OTUs were active prior to the enrichment, and at any point in time a significant fraction of functionally similar clades may have only been present at low densities (Shade *et al*., 2014). Furthermore, subtle partitioning along additional non-functional axes such as moisture or pH may create micro-niches that enable the long-term coexistence of functionally similar populations, particularly in spatially or temporally heterogenous environments. For example, the coexistence of hundreds of sub-populations of the marine cyanobacterium *Prochlorococcus* is likely enabled by subtle niche differentiation such as adaptations to different nutrient availabilities (Kashtan *et al*., 2014). The role of neutrality in natural microbial communities and its proper reconciliation with niche theory remain controversial. Nevertheless, our work shows that approximate neutrality within ecological niches can explain several patterns of microbial community assembly in engineered environments and should also be considered when interpreting the dynamics of natural microbial communities.

Experimental procedures

Computational framework

Model calibration, simulations and statistical analysis were performed using MCM (Microbial Community Modeler), a mathematical and computational framework that we developed for modelling microbial ecosystems (Louca and Doebeli, 2015, in press). MCM combines FBA-based cell models with a dynamical environment that influences, and is influenced by, microbial metabolism. The combination of FBA with a varying environmental metabolite pool is known as dynamic flux balance analysis (DFBA) (Mahadevan *et al*., 2002; Chiu *et al*., 2014; Harcombe *et al*., 2014) and has been shown to be a promising approach to microbial ecological modelling (Meadows *et al*., 2010; Chiu *et al*., 2014; Harcombe *et al*., 2014; Louca and Doebeli, 2015, in press). MCM can accommodate microbial community models with arbitrary environmental variables and metabolite exchange kinetics. For example, environmental variables may be stochastic processes (e.g. representing climate fluctuations), or specified using measured data (e.g. pH in bioreactor experiments). Metabolite uptake and export rate limits can be arbitrary functions of metabolite concentrations or environmental variables. Similar interdependencies are possible for reaction rate limits, thus allowing the inclusion of inhibitory or regulatory mechanisms (Covert *et al*., 2008). Metabolite concentrations can be explicitly specified, e.g. using measured time series, or depend dynamically on microbial export and other external fluxes.

MCM keeps track of a multitude of output variables such as cell concentrations, reaction rates, metabolite concentrations and metabolite exchange rates. Model predictions can then be compared with time series from experiments or environmental surveys, such as rate measurements, chemical profiles or optical cell densities. Reciprocally, time series data can be used to automatically calibrate unknown model parameters, e.g. using least-squares fitting or maximum likelihood estimation (e.g. Fig. 1, see details below). Because MCM can calibrate unknown measurement units, raw uncalibrated data (e.g. optical cell densities with no calibration to colony-forming units) can also be used. MCM was recently validated using laboratory experiments with bacterial communities (Louca and Doebeli, 2015, in press). MCM is Open Source and available at http://www.zoology.ubc.ca/MCM.

Construction of the cell models

The metabolism of each cell was modelled using FBA with optimization of biomass synthesis (Orth *et al*., 2010). The cell-internal reaction networks of the AOB and NOB are based on the core metabolic models published by Poughon and colleagues (2001) and Perez-Garcia and colleagues (2014). More precisely, the biomass synthesis functions of both cell types are taken from Perez-Garcia and colleagues (2014), the energy metabolism of AOB is adopted from Perez-Garcia and colleagues (2014) and the energy metabolism of NOB is adopted from Poughon and colleagues (2001). Assimilatory nitrite reduction to ammonium, required for biomass synthesis, was added to NOB (Starkenburg *et al*., 2006). The constructed AOB and NOB models are comprised of 16 and 11 reactions respectively (see Supporting Information S2 for details). The nitrogen substrate half-saturation constants were set to 26 μM NH_3 for the AOB template according to Suzuki and colleagues (1974) and to 229 μM NO_2^- for the NOB template according to Remacle and De Leval (1978). Cell masses were set to 3×10^{-13} g dW cell^{-1} for the AOB and 4×10^{-13} g dW cell^{-1} for the NOB, according to Keen and Prosser (1987).

Calibration of the template cell models

The maximum cell-specific substrate uptake rates for the AOB and NOB templates (V_{max,NH_4^+} and V_{max,NO_3^-} respectively) were calibrated using time series from a previous experiment with an ammonium-batch-fed nitrifying bioreactor by de Boer and Laanbroek (1989), inoculated with strains of the AOB *Nitrosospira* and NOB *Nitrobacter* genera. For the calibration, our bioreactor model was adjusted to de Boer and Laanbroek's experiment (Fig. 1A): The initial ammonium concentration was set to 0.916 mM, nitrite and nitrate were initially absent, the pH was set to the reported profile and oxygen was assumed to be non-limiting.

We used the reported concentration profiles of the gradually depleted ammonium (Fig. 1B) and produced nitrate (Fig. 1C) to calibrate V_{max,NH_4^+} and V_{max,NO_3^-} via maximum likelihood estimation (Eliason, 1993). This approach estimates unknown parameters by maximizing the likelihood of observing the available data, given a particular candidate choice of parameter values. Maximum likelihood estimation is widely used in statistical inference such as multilinear regression, computational phylogenetics and modelling in physics (Lyons, 1986). In our case, the likelihood of the data was calculated on the basis of a mixed deterministic-stochastic structure, in which the deterministic part is given by the microbial community model, and errors are assumed to be normally distributed. The likelihood was maximized using a subspace-searching simplex algorithm (SBPLX; Johnson, 2014), which uses repeated simulations and gradual exploration of parameter space and is integrated into MCM (Louca and Doebeli, 2015, in press). To reduce the possibility of only reaching a local maximum, fitting was repeated 100 times using random initial parameter values and the best fit among all 100 runs was used. While some fitting runs reached alternative local maxima, the best overall fit was reached in most cases. This procedure yielded the fitted values $V_{max,NH_4^+} = 6.48\times10^{-13}\text{mol } NH_3/\text{cell/d}$ and $V_{max,NO_2^-} = 7.31\times10^{-13}\text{mol } NO_2^-/\text{cell/d}$, which are consistent with the literature (Prosser, 2005).

Nitrifying membrane bioreactor model

Using the calibrated AOB and NOB template cell models, we constructed a model of an ammonium-fed nitrifying membrane bioreactor similar to the one described by Wittebolle and colleagues (2008). The hydraulic turnover rate for all metabolites was 0.672 per day, ammonium input was 7.14 mM per day and pH was fixed to 7.4. The input medium was assumed to be sterile and to contain micronutrients in sufficient amounts for autotrophic growth via nitrification (Wittebolle *et al*., 2008; Dumont *et al*., 2009). The bioreactor medium was assumed to be well mixed. Microbial communities started with an equal number of AOB and NOB strains, each with an initial density of 10^7 cells L^{-1}. Cell death was modelled as exponential decay (see Supporting Information S2 for details).

Each strain was a random variation of the calibrated template cell models, with physiological parameters chosen as follows: Substrate uptake kinetic parameters, i.e. the maximum cell-specific nitrogen substrate uptake rates (V_{max}) and substrate affinities (α; Aksnes and Cao, 2011), were randomly and uniformly chosen within an interval ranging an order of magnitude above and an order of magnitude below the template values. To account for the typically assumed trade-off between V_{max} and α, these parameters were multiplied by a factor κ and $(1 - \kappa)$, respectively, where κ was chosen randomly between 0 and 1 for each strain (Smith *et al*., 2009). Cell life times were randomly chosen within 50–100 days for each strain according to typical nitrifier decay rates (Alleman and Preston, 1991).

Perturbations were modelled as a temporary increase in mortality rates, such that after 1 day each cell population declines by some random factor, chosen log-uniformly and independently for each strain within the interval $[1, 10^{12}]$.

Statistics of community convergence

The distance between two community compositions was expressed using the Bray–Curtis dissimilarity, which is well established in the ecological literature (Legendre and Legendre, 1998). The maximum dissimilarity between any two communities is 100%, whereas identical communities have a dissimilarity of 0%. The convergence of the bioreactor community was examined by calculating its dissimilarity to the steady composition established after a long time. This dissimilarity curve is typically decreasing in time because communities eventually converge to a steady composition in which each metabolic niche is occupied by a single strain. A steeper curve implies a faster convergence. Following inoculation, the dissimilarity curve depends on the particular strains present in the community, which are chosen randomly for each simulation. The resulting probability distribution of the dissimilarity curves (Figs 2E,F and 3E,F) was estimated using 100 repeated random simulations of the model.

Acknowledgements

S.L. acknowledges the financial support of the PIMS IGTC for Mathematical Biology as well as the Department of Mathematics, UBC. S.L. and M.D. acknowledge the support of NSERC. The authors thank Andrew H. Loudon for comments. No conflict of interest declared.

References

Aksnes, D.L., and Cao, F.J. (2011) Inherent and apparent traits in microbial nutrient uptake. *Mar Ecol Prog Ser* **440:** 41–51.

Alleman, J.E., and Preston, K. (1991) Behavior and physiology of nitrifying bacteria. *Proceedings of the Second Annual Conference on Commercial Aquaculture, CES*, volume 240, pp. 1–13.

Anthonisen, A.C., Loehr, R.C., Prakasam, T.B.S., and Srinath, E.G. (1976) Inhibition of nitrification by ammonia and nitrous acid. *J Water Pollut Control Fed* **48:** 835–852.

Antolli, P., and Liu, Z. (2012) *Bioreactors: Design, Properties, and Applications*. Biochemistry Research Trends Series. New York, NY, USA, Nova Science Publishers.

Ayarza, J., Guerrero, L., and Erijman, L. (2010) Nonrandom assembly of bacterial populations in activated sludge flocs. *Microb Ecol* **59:** 436–444.

de Boer, W., and Laanbroek, H. (1989) Ureolytic nitrification at low pH by *Nitrosospira* spec. *Arch Microbiol* **152:** 178–181.

Briones, A., and Raskin, L. (2003) Diversity and dynamics of microbial communities in engineered environments and their implications for process stability. *Curr Opin Biotechnol* **14:** 270–276.

Burgard, A.P., and Maranas, C.D. (2003) Optimization-based framework for inferring and testing hypothesized metabolic objective functions. *Biotechnol Bioeng* **82:** 670–677.

Burke, C., Steinberg, P., Rusch, D., Kjelleberg, S., and Thomas, T. (2011) Bacterial community assembly based on functional genes rather than species. *Proc Natl Acad Sci USA* **108:** 14288–14293.

Caruso, T., Chan, Y., Lacap, D.C., Lau, M.C.Y., McKay, C.P., and Pointing, S.B. (2011) Stochastic and deterministic processes interact in the assembly of desert microbial communities on a global scale. *ISME J* **5:** 1406–1413.

Chesson, P. (2000) Mechanisms of maintenance of species diversity. *Annu Rev Ecol Syst* **31:** 343–366.

Chiu, H.C., Levy, R., and Borenstein, E. (2014) Emergent biosynthetic capacity in simple microbial communities. *PLoS Comput Biol* **10:** e1003695.

Connell, J.H. (1978) Diversity in tropical rain forests and coral reefs. *Science* **199:** 1302–1310.

Covert, M.W., Xiao, N., Chen, T.J., and Karr, J.R. (2008) Integrating metabolic, transcriptional regulatory and signal transduction models in *Escherichia coli*. *Bioinformatics* **24:** 2044–2050.

Doak, D.F., Bigger, D., Harding, E., Marvier, M., O'Malley, R., and Thomson, D. (1998) The statistical inevitability of stability-diversity relationships in community ecology. *Am Nat* **151:** 264–276.

Doolittle, W.F., and Zhaxybayeva, O. (2010) Metagenomics and the units of biological organization. *Bioscience* **60:** 102–112.

Duarte, N.C., Herrgård, M.J., and Palsson, B.Ø. (2004) Reconstruction and validation of *Saccharomyces cerevisiae* iND750, a fully compartmentalized genome-scale metabolic model. *Genome Res* **14:** 1298–1309.

Dumont, M., Harmand, J., Rapaport, A., and Godon, J.J. (2009) Towards functional molecular fingerprints. *Environ Microbiol* **11:** 1717–1727.

Eliason, S.R. (1993) *Maximum Likelihood Estimation: Logic and Practice*. Newbury Park, CA, USA: SAGE Publications.

Falkowski, P.G., Fenchel, T., and Delong, E.F. (2008) The microbial engines that drive earth's biogeochemical cycles. *Science* **320:** 1034–1039.

Feist, A.M., and Palsson, B.O. (2010) The biomass objective function. *Curr Opin Microbiol* **13:** 344–349.

Fernández, A., Huang, S., Seston, S., Xing, J., Hickey, R., Criddle, C., *et al*. (1999) How stable is stable? Function versus community composition. *Appl Environ Microbiol* **65:** 3697–3704.

Fernandez, A.S., Hashsham, S.A., Dollhopf, S.L., Raskin, L., Glagoleva, O., Dazzo, F.B., *et al*. (2000) Flexible community structure correlates with stable community function in methanogenic bioreactor communities perturbed by glucose. *Appl Environ Microbiol* **66:** 4058–4067.

Freilich, S., Zarecki, R., Eilam, O., Segal, E.S., Henry, C.S., Kupiec, M., *et al*. (2011) Competitive and cooperative metabolic interactions in bacterial communities. *Nat Commun* **2:** 589.

Frigaard, N.U., Martinez, A., Mincer, T.J., and DeLong, E.F. (2006) Proteorhodopsin lateral gene transfer between marine planktonic *Bacteria* and *Archaea*. *Nature* **439:** 847–850.

Frossard, A., Gerull, L., Mutz, M., and Gessner, M.O. (2012) Disconnect of microbial structure and function: enzyme activities and bacterial communities in nascent stream corridors. *ISME J* **6:** 680–691.

Gentile, M., Yan, T., Tiquia, S., Fields, M., Nyman, J., Zhou, J., *et al*. (2006) Stability in a denitrifying fluidized bed reactor. *Microb Ecol* **52:** 311–321.

Gevers, D., Cohan, F.M., Lawrence, J.G., Spratt, B.G., Coenye, T., Feil, E.J., *et al*. (2005) Re-evaluating prokaryotic species. *Nat Rev Microbiol* **3:** 733–739.

Gianchandani, E.P., Oberhardt, M.A., Burgard, A.P., Maranas, C.D., and Papin, J.A. (2008) Predicting biological system objectives de novo from internal state measurements. *BMC Bioinformatics* **9:** 43.

Gilbert, J., Meyer, F., Antonopoulos, D.A., Balaji, P., Brown, C.T., Brown, C.T., *et al*. (2010) Meeting report: the terabase metagenomics workshop and the vision of an Earth microbiome project. *Stand Genomic Sci* **3:** 243–248.

Graham, D.W., Knapp, C.W., Van Vleck, E.S., Bloor, K., Lane, T.B., and Graham, C.E. (2007) Experimental demonstration of chaotic instability in biological nitrification. *ISME J* **1:** 385–393.

Harcombe, W.R., Delaney, N.F., Leiby, N., Klitgord, N., and Marx, C.J. (2013) The ability of flux balance analysis to predict evolution of central metabolism scales with the initial distance to the optimum. *PLoS Comput Biol* **9:** e1003091.

Harcombe, W.R., Riehl, W.J., Dukovski, I., Granger, B.R., Betts, A., Lang, A.H., *et al*. (2014) Metabolic resource allocation in individual microbes determines ecosystem interactions and spatial dynamics. *Cell Rep* **7:** 1104–1115.

Hardin, G. (1960) The competitive exclusion principle. *Science* **131:** 1292–1297.

Hastings, A. (2004) Transients: the key to long-term ecological understanding? *Trends Ecol Evol* **19:** 39–45.

Hawley, A.K., Brewer, H.M., Norbeck, A.D., Paša-Tolić, L., and Hallam, S.J. (2014) Metaproteomics reveals differential modes of metabolic coupling among ubiquitous oxygen minimum zone microbes. *Proc Natl Acad Sci USA* **111:** 11395–11400.

Hérault, B. (2007) Reconciling niche and neutrality through the emergent group approach. *Perspect Plant Ecol Evol Syst* **9:** 71–78.

Hubbell, S.P. (2005) Neutral theory in community ecology and the hypothesis of functional equivalence. *Funct Ecol* **19:** 166–172.

Jin, Q., Roden, E.E., and Giska, J.R. (2013) Geomicrobial kinetics: extrapolating laboratory studies to natural environments. *Geomicrobiol J* **30:** 173–185.

Johnson, S.G. (2014) The nlopt nonlinear-optimization package. [WWW document]. URL http://ab-initio.mit.edu/nlopt.

Kashtan, N., Roggensack, S.E., Rodrigue, S., Thompson, J.W., Biller, S.J., Coe, A., *et al*. (2014) Single-cell genomics reveals hundreds of coexisting subpopulations in wild *Prochlorococcus*. *Science* **344:** 416–420.

Kaspar, H., and Wuhrmann, K. (1977) Product inhibition in sludge digestion. *Microb Ecol* **4:** 241–248.

Keen, G., and Prosser, J. (1987) Steady state and transient growth of autotrophic nitrifying bacteria. *Arch Microbiol* **147:** 73–79.

Kim, T.S., Jeong, J.Y., Wells, G., and Park, H.D. (2013) General and rare bacterial taxa demonstrating different temporal dynamic patterns in an activated sludge bioreactor. *Appl Microbiol Biotechnol* **97:** 1755–1765.

Klitgord, N., and Segrè, D. (2010) Environments that induce synthetic microbial ecosystems. *PLoS Comput Biol* **6:** e1001002.

Legendre, P., and Legendre, L. (1998) *Numerical Ecology. Developments in Environmental Modelling*, 2nd edn. Amsterdam: Elsevier Science B.V.

Lehman, C.L., and Tilman, D. (2000) Biodiversity, stability, and productivity in competitive communities. *Am Nat* **156:** 534–552.

Loreau, M., Naeem, S., Inchausti, P., Bengtsson, J., Grime, J., Hector, A., *et al*. (2001) Biodiversity and ecosystem functioning: Current knowledge and future challenges. *Science* **294:** 804–808.

Louca, S., and Doebeli, M. (2015) Calibration and analysis of genome-based models for microbialecology. *eLife* (In press).

Lyons, L. (1986) *Statistics for Nuclear and Particle Physicists*. Cambridge, UK: Cambridge University Press.

McGuinness, L.M., Salganik, M., Vega, L., Pickering, K.D., and Kerkhof, L.J. (2006) Replicability of bacterial communities in denitrifying bioreactors as measured by PCR/T-RFLP analysis. *Environ Sci Technol* **40:** 509–515.

Mahadevan, R., Edwards, J.S., and Doyle, F.J., III (2002) Dynamic flux balance analysis of diauxic growth in *Escherichia coli*. *Biophys J* **83:** 1331–1340.

Martens-Habbena, W., Berube, P.M., Urakawa, H., de la Torre, J.R., and Stahl, D.A. (2009) Ammonia oxidation kinetics determine niche separation of nitrifying *Archaea* and *Bacteria*. *Nature* **461:** 976–979.

Meadows, A.L., Karnik, R., Lam, H., Forestell, S., and Snedecor, B. (2010) Application of dynamic flux balance analysis to an industrial *Escherichia coli* fermentation. *Metab Eng* **12:** 150–160.

Ofiţeru, I.D., Lunn, M., Curtis, T.P., Wells, G.F., Criddle, C.S., Francis, C.A., *et al*. (2010) Combined niche and neutral effects in a microbial wastewater treatment community. *Proc Natl Acad Sci USA* **107:** 15345–15350.

Orth, J.D., Thiele, I., and Palsson, B.O. (2010) What is flux balance analysis? *Nat Biotechnol* **28:** 245–248.

Perez-Garcia, O., Villas-Boas, S.G., Swift, S., Chandran, K., and Singhal, N. (2014) Clarifying the regulation of NO/N_2O production in *Nitrosomonas europaea* during anoxic–oxic transition via flux balance analysis of a metabolic network model. *Water Res* **60:** 267–277.

Poughon, L., Dussap, C.G., and Gros, J.B. (2001) Energy model and metabolic flux analysis for autotrophic nitrifiers. *Biotechnol Bioeng* **72:** 416–433.

Prosser, J. (2005) *Nitrogen in Soils: Nitrification*. In *Encyclopedia of Soils in the Environment*. Hillel, D. (ed.) Oxford, UK: Elsevier, pp. 31–39.

Raes, J., Letunic, I., Yamada, T., Jensen, L.J., and Bork, P. (2011) Toward molecular trait-based ecology through integration of biogeochemical, geographical and metagenomic data. *Mol Syst Biol* **7:** 473.

Raymond, J., Siefert, J.L., Staples, C.R., and Blankenship, R.E. (2004) The natural history of nitrogen fixation. *Mol Biol Evol* **21:** 541–554.

Reed, D.C., Algar, C.K., Huber, J.A., and Dick, G.J. (2014) Gene-centric approach to integrating environmental genomics and biogeochemical models. *Proc Natl Acad Sci USA* **111:** 1879–1884.

Remacle, J., and De Leval, J. (1978) *Approaches to Nitrification in a River*. Washington: American Society for Microbiology, pp. 352–356.

Schink, B., and Stams, A. (2006) Syntrophism among prokaryotes. In *The Prokaryotes*. Dworkin, M., Falkow, S., Rosenberg, E., Schleifer, K.H., and Stackebrandt, E. (eds). New York, NY, USA: Springer, pp. 309–335.

Schneider, S. (2004) *Scientists Debate Gaia: The Next Century*. Cambridge, Massachusetts: MIT Press.

Segrè, D., Vitkup, D., and Church, G.M. (2002) Analysis of optimality in natural and perturbed metabolic networks. *Proc Natl Acad Sci USA* **99:** 15112–15117.

Shade, A., Peter, H., Allison, S.D., Baho, D.L., Berga, M., Bürgmann, H., *et al*. (2012) Fundamentals of microbial community resistance and resilience. *Front Microbiol* **3:** 417.

Shade, A., Jones, S.E., Caporaso, J.G., Handelsman, J., Knight, R., Fierer, N., *et al*. (2014) Conditionally rare taxa disproportionately contribute to temporal changes in microbial diversity. *mBio* **5:** e01371–14.

Shapiro, O.H., and Kushmaro, A. (2011) Bacteriophage ecology in environmental biotechnology processes. *Curr Opin Biotechnol* **22:** 449–455.

Sheintuch, M., Tartakovsky, B., Narkis, N., and Rebhun, M. (1995) Substrate inhibition and multiple states in a continuous nitrification process. *Water Res* **29:** 953–963.

Smith, S.L., Yamanaka, Y., Pahlow, M., and Oschlies, A. (2009) Optimal uptake kinetics: physiological acclimation explains the pattern of nitrate uptake by phytoplankton in the ocean. *Mar Ecol Prog Ser* **384:** 1–12.

Sommer, U. (1984) The paradox of the plankton: fluctuations of phosphorus availability maintain diversity of phytoplankton in flow-through cultures. *Limnol Oceanogr* **29:** 633–636.

Stackebrandt, E., Frederiksen, W., Garrity, G.M., Grimont, P.A.D., Kämpfer, P., Maiden, M.C.J., *et al*. (2002) Report of the ad hoc committee for the re-evaluation of the species definition in bacteriology. *Int J Syst Evol Microbiol* **52:** 1043–1047.

Starkenburg, S.R., Chain, P.S.G., Sayavedra-Soto, L.A., Hauser, L., Land, M.L., Larimer, F.W., *et al*. (2006) Genome sequence of the chemolithoautotrophic nitrite-oxidizing bacterium *Nitrobacter winogradskyi* nb-255. *Appl Environ Microbiol* **72:** 2050–2063.

Sundh, I., Carlsson, H., Nordberg, Å., Hansson, M., and Mathisen, B. (2003) Effects of glucose over loading on microbial community structure and biogas production in a laboratory-scale anaerobic digester. *Bioresour Technol* **89:** 237–243.

Suzuki, I., Dular, U., and Kwok, S.C. (1974) Ammonia or ammonium ion as substrate for oxidation by *Nitrosomonas europaea* cells and extracts. *J Bacteriol* **120:** 556–558.

Thingstad, T.F. (2000) Elements of a theory for the mechanisms controlling abundance, diversity, and biogeochemical role of lytic bacterial viruses in aquatic systems. *Limnol Oceanogr* **45:** 1320–1328.
Tilman, D. (1982) *Resource Competition and Community Structure*. Princeton, NJ, USA: Princeton University Press.
Tilman, D. (1996) Biodiversity: population versus ecosystem stability. *Ecology* **77:** 350–363.
Tilman, D., Lehman, C.L., and Bristow, C.E. (1998) Diversity-stability relationships: statistical in evitability or ecological consequence? *Am Nat* **151:** 277–282.
Vanwonterghem, I., Jensen, P.D., Dennis, P.G., Hugenholtz, P., Rabaey, K., and Tyson, G.W. (2014) Deterministic processes guide long-term synchronised population dynamics in replicate anaerobic digesters. *ISME J* **8:** 2015–2028.
Wang, X., Wen, X., Yan, H., Ding, K., Zhao, F., and Hu, M. (2011) Bacterial community dynamics in a functionally stable pilot-scale wastewater treatment plant. *Bioresour Technol* **102:** 2352–2357.
Ward, D.M., Cohan, F.M., Bhaya, D., Heidelberg, J.F., Kuhl, M., and Grossman, A. (2007) Genomics, environmental genomics and the issue of microbial species. *Heredity* **100:** 207–219.
Welch, R.A., Burland, V., Plunkett, G., Redford, P., Roesch, P., Rasko, D., *et al*. (2002) Extensive mosaic structure revealed by the complete genome sequence of uropathogenic *Escherichia coli*. *Proc Natl Acad Sci USA* **99:** 17020–17024.
Wittebolle, L., Vervaeren, H., Verstraete, W., and Boon, N. (2008) Quantifying community dynamics of nitrifiers in functionally stable reactors. *Appl Environ Microbiol* **74:** 286–293.
Wittebolle, L., Verstraete, W., and Boon, N. (2009) The inoculum effect on the ammonia-oxidizing bacterial communities in parallel sequential batch reactors. *Water Res* **43:** 4149–4158.
Xing, J., Criddle, C., and Hickey, R. (1997) Long-term adaptive shifts in anaerobic community structure in response to a sustained cyclic substrate perturbation. *Microb Ecol* **33:** 50–58.
Yin, B., Crowley, D., Sparovek, G., De Melo, W.J., and Borneman, J. (2000) Bacterial functional redundancy along a soil reclamation gradient. *Appl Environ Microbiol* **66:** 4361–4365.
Zaikova, E., Walsh, D.A., Stilwell, C.P., Mohn, W.W., Tortell, P.D., and Hallam, S.J. (2010) Microbial community dynamics in a seasonally anoxic fjord: Saanich Inlet, British Columbia. *Environ Microbiol* **12:** 172–191.
Zumstein, E., Moletta, R., and Godon, J.J. (2000) Examination of two years of community dynamics in an anaerobic bioreactor using fluorescence polymerase chain reaction (PCR) single-strand conformation polymorphism analysis. *Environ Microbiol* **2:** 69–78.

Supporting information

Additional Supporting Information may be found in the online version of this article at the publisher's web-site:

Mathematical details of the competition model introduced at the beginning of this article are available as Supporting Information S1. Details on the bioreactor model, including the AOB and NOB reaction networks, can be found in Supporting Information S2. The model files for the batch-fed bioreactor along with the MCM script required for simulation and calibration are available as Supporting Information S3 or on the official MCM website, http://www.zoology.ubc.ca/MCM. The model files and simulation script for the continuous-flow bioreactor are available as Supporting Information S4 or on the official MCM website.

Supporting Information S1. Elaboration on the competition model.
Supporting Information S2. Details on the bioreactor model.
Supporting Information S3. Model files for the batch-fed bioreactor and MCM script for simulation and calibration.
Supporting Information S4. Model files and simulation script for the continuous-flow bioreactor.

Transient dynamics of competitive exclusion in microbial communities
- Supporting Information S1 -

Stilianos Louca[1] and Michael Doebeli[2,3]

[1]*Biodiversity Research Centre, University of British Columbia, Vancouver, BC, V6T 1Z4, Canada, louca@zoology.ubc.ca*
[2]*Department of Zoology, University of British Columbia, Vancouver, BC, V6T 1Z4 Canada,*
[3]*Department of Mathematics, University of British Columbia, Vancouver BC, V6T 1Z2 Canada*

S1 Elaboration on the competition model

Below we elaborate on the competition model in the main article. We consider the total cell density $N = \sum_i N_i$ and the relative cell densities $\eta_i = N_i/N$. Using the community-average quantities

$$\overline{\beta\Phi} = \sum_i \eta_i \beta_i \Phi_i,\ \overline{\lambda} = \sum_i \eta_i \lambda_i,\ \overline{\Phi} = \sum_i \eta_i \Phi_i \tag{S.1}$$

it is straightforward to derive the dynamics

$$\frac{dR}{dt} = f_o - N\overline{\Phi}(R) \tag{S.2}$$

for the resource concentration. Similarly, starting with

$$\frac{dN}{dt} = \sum_i \frac{dN_i}{dt} \tag{S.3}$$

and using the original model equations for the N_i one quickly arrives at

$$\frac{dN}{dt} = N\left(\overline{\beta\Phi}(R) - \overline{\lambda}\right). \tag{S.4}$$

Furthermore, by using the product rule

$$\frac{d\eta_i}{dt} = \frac{1}{N}\frac{dN_i}{dt} - \frac{N_i}{N^2}\frac{dN}{dt} \tag{S.5}$$

and inserting Eq. (S.4) one finds that

$$\frac{d\eta_i}{dt} = \eta_i\big[(\beta_i\Phi_i - \lambda_i) - (\overline{\beta\Phi} - \overline{\lambda})\big]. \tag{S.6}$$

Note that the dynamics of N and R are determined by the community-average growth kinetics. In contrast, relative cell densities change at rates that depend on the deviation of individual growth kinetics from the community average. Furthermore, one can always write

$$\beta_i \Phi_i - \lambda_i = \left(\overline{\beta\Phi} - \overline{\lambda}\right)(1 + \varepsilon_i), \tag{S.7}$$

where ε_i accounts for the relative deviation of individual growth kinetics from the community average. Then Eq. (S.6) becomes

$$\frac{d\eta_i}{dt} = \varepsilon_i \cdot \eta_i(\overline{\beta\Phi} - \overline{\lambda}), \tag{S.8}$$

as given in the main article.

Transient dynamics of competitive exclusion in microbial communities
- Supporting Information S2 -

Stilianos Louca[1] and Michael Doebeli[2,3]

[1]*Biodiversity Research Centre, University of British Columbia, Vancouver, BC, V6T 1Z4, Canada, louca@zoology.ubc.ca*
[2]*Department of Zoology, University of British Columbia, Vancouver, BC, V6T 1Z4 Canada,*
[3]*Department of Mathematics, University of British Columbia, Vancouver BC, V6T 1Z2 Canada*

S2 Details on the bioreactor model

S2.1 Construction of cell models

The reaction networks for the two cell types, AOB and NOB, only include core energy metabolism and biomass synthesis (production of ATP and NADH via nitrification and biosynthesis via consumption of ATP and NADH). The biomass synthesis functions of both cell types are taken from [4], assuming that biomass stoichiometry is similar for *Nitrosomonas* (AOB) and *Nitrobacter* (NOB) cells. In particular, energy-to-biomass conversion coefficients (ATP & NADH to g dry weight) were experimentally calibrated by [4]. The energy metabolism of AOB is taken from [4]. Note that the original published AOB model had 17 reactions related to energy metabolism (Table S1 in [4]). One of these reactions, "NO1", was merely a trivial conversion reaction and was thus merged with the rest. The remaining reactions in the AOB model by [4] were pure transport reactions and are implicitly included in the MCM model (but not referred to as "reactions"). The energy metabolism of NOB is taken from [5]. Assimilatory nitrite reduction to ammonium, required for biomass synthesis but not included in the original reaction network by [5], was added to NOB according to [7]. Uptake kinetic parameters for $\mathrm{NH_3}.\mathrm{NH_4}$ and $\mathrm{HNO_2}.\mathrm{NO_2}$, as well as cell life times and cell masses were chosen as described in the main article. Below we provide an overview of all considered metabolites and reactions. Please consult the references by the reactions for details. The complete model and simulation script are available as separate supplementary material.

S2.2 Metabolites

- ADP (adenosine diphosphate)
- ATP (adenosine triphosphate)

- CO_2 (carbon dioxide)
- $\mathrm{Cytc_{550ox}}$ (class I cytochrome c550, oxidized)
- $\mathrm{Cytc_{550red}}$ (class I cytochrome c550, reduced)
- $\mathrm{Cytc_{552ox}}$ (class I cytochrome c552, oxidized)
- $\mathrm{Cytc_{552red}}$ (class I cytochrome c552, reduced)
- $\mathrm{Cytc_{554ox}}$ (class I cytochrome c554, oxidized)
- $\mathrm{Cytc_{554red}}$ (class I cytochrome c554, reduced)
- $\mathrm{H_c}$ (hydrogen, cytosol)
- $\mathrm{H_p}$ (hydrogen, periplasm)
- H_2O (water)
- $\mathrm{NH_3.NH_4}$ (ammonia + ammonium)
- NH_3 (purely extracellular, ammonia, depending on $\mathrm{NH_3.NH_4}$ and pH, see notes below)
- NH_4 (purely extracellular, ammonium, depending on $\mathrm{NH_3.NH_4}$ and pH, see notes below)
- $\mathrm{HNO_2.NO_2}$ (nitrite + nitrous acid)
- NO_2 (purely extracellular, nitrite, depending on $\mathrm{HNO_2.NO_2}$ and pH)
- $\mathrm{HNO_3.NO_3}$ (nitrate + nitric acid)
- NO_3 (purely extracellular, nitrate, depending on $\mathrm{HNO_3.NO_3}$ and pH)
- N_2O (nitrous oxide)
- NAD (oxidized nicotinamide adenine dinucleotide)
- NADH (Reduced nicotinamide adenine dinucleotide)
- NH_2OH (hydroxylamine)
- NO (nitric oxide)
- NOH (nitroxyle)
- O_2 (oxygen)
- Pi (inorganic phosphate)
- protein
- UQ (ubiquinone)

- UQH_2 (ubiquinol)
- maint (formal maintenance requirements, in ATP-equivalents)
- Q_8H_2 (ubiquinol-8)
- Q_8 (ubiquinone-8)
- Cyt_{554e} (ferrocytochrome c554)
- Cyt_{554} (ferricytochrome c554)
- Cyt_{552me} (membrane ferrocytochrome)
- Cyt_{552m} (ferricytochrome c552)
- Cyt_{552e} (periplasmic ferrocytochrome c552)
- Cyt_{552} (ferricytochrome c552)

Note that in the model ammonium (NH_4) is assumed to be at dissociation equilibrium with ammonia (NH_3), determined by the pH and the acid dissociation constant 5.69×10^{-10} M at standard temperature [2]. pH was either adjusted to measurements for the batch reactor [3], or to constant 7.4 for the membrane continuous-flow reactor [9]. The total concentration of ammonium and ammonia is represented in the model by $NH_3.NH_4$, and depends on the rate of ammonium input, the hydraulic dilution rate and microbial consumption. A similar formalism was applied to nitrite and nitrate.

S2.3 Reaction network for AOB

R_biomass [4] (biomass coefficient 113 g dW/mol, modified to include CO_2 consumption):

$$\begin{aligned} &15\ \mathrm{ATP} + 12\ \mathrm{NADH} + 0.25\ \mathrm{protein} + 32\ \mathrm{maint} + 5\ \mathrm{CO_2} + 7\ \mathrm{H_c} \\ &\rightarrow 15\ \mathrm{ADP} + 10\ \mathrm{NAD} + 15\ \mathrm{Pi} + 4\ \mathrm{O_2} \end{aligned} \tag{S.1}$$

R_maint [4] (maintenance ATP consumption):

$$\mathrm{ATP} + \mathrm{H_2O} \rightarrow \mathrm{ADP} + \mathrm{Pi} + \mathrm{H_c} + \mathrm{maint} \tag{S.2}$$

R_protein [4] (protein synthesis via ATP consumption):

$$8.9\ \mathrm{ATP} + 4\ \mathrm{NH_3.NH_4} \rightarrow 8.9\ \mathrm{ADP} + 8.9\ \mathrm{Pi} + 8.9\ \mathrm{H_c} + \mathrm{protein} \tag{S.3}$$

R_amo [4]:

$$\mathrm{NH_3.NH_4} + \mathrm{O_2} + \mathrm{Q_8H_2} \rightarrow \mathrm{NH_2OH} + \mathrm{H_2O} + \mathrm{Q_8} \tag{S.4}$$

R_HAO_NOH [4]:

$$\mathrm{NH_2OH} + \mathrm{Cyt_{554}} \rightarrow \mathrm{NOH} + \mathrm{Cyt_{554e}} + 2\ \mathrm{H_p} \tag{S.5}$$

R_HAO_NO [4]:

$$\mathrm{NOH} + 0.5\ \mathrm{Cyt_{554}} \rightarrow \mathrm{NO} + 0.5\ \mathrm{Cyt_{554e}} + \mathrm{H_p} \tag{S.6}$$

R_HAO_hno2 [4]:

$$\mathrm{NO} + 0.5\ \mathrm{Cyt_{554}} + \mathrm{H_2O} \rightarrow \mathrm{HNO_2.NO_2} + 0.5\ \mathrm{Cyt_{554e}} + \mathrm{H_p} \tag{S.7}$$

R_Cyt_554 [4]:

$$\mathrm{Cyt_{554e}} + \mathrm{Cyt_{552m}} \rightarrow \mathrm{Cyt_{552me}} + \mathrm{Cyt_{554}} \tag{S.8}$$

R_Q_8H_2_synt [4]:

$$\mathrm{Q_8} + \mathrm{Cyt_{552me}} + 2\ \mathrm{H_p} \rightarrow \mathrm{Q_8H_2} + \mathrm{Cyt_{552m}} \tag{S.9}$$

R_NADH_synt [4]:

$$\mathrm{NAD} + \mathrm{Q_8H_2} + 2\ \mathrm{H_p} \rightarrow \mathrm{NADH} + \mathrm{Q_8} + 3\ \mathrm{H_c} \tag{S.10}$$

R_Cytbc1 [4]:

$$\mathrm{Q_8H_2} + 2\ \mathrm{Cyt_{552}} \rightarrow 2\ \mathrm{H_p} + \mathrm{Q_8} + 2\ \mathrm{Cyt_{552e}} \tag{S.11}$$

R_Cytaa3 [4]:

$$0.5\ \mathrm{O_2} + 4\ \mathrm{H_c} + 2\ \mathrm{Cyt_{552e}} \rightarrow \mathrm{H_2O} + 2\ \mathrm{H_p} + 2\ \mathrm{Cyt_{552}} \tag{S.12}$$

R_CytP460 [4]:

$$\begin{aligned} &0.5\ \mathrm{NH_2OH} + 0.5\ \mathrm{NO} + 2.5\ \mathrm{Cyt_{552}} + \mathrm{H_2O} \\ &\rightarrow \mathrm{HNO_2.NO_2} + 2.5\ \mathrm{Cyt_{552e}} + 2.5\ \mathrm{H_p} \end{aligned} \tag{S.13}$$

R_nir [4]:

$$\mathrm{HNO_2.NO_2} + \mathrm{Cyt_{552e}} + \mathrm{H_p} \rightarrow \mathrm{NO} + \mathrm{Cyt_{552}} + \mathrm{H_2O} \tag{S.14}$$

R_nor [4]:

$$\mathrm{NO} + \mathrm{Cyt_{552e}} + \mathrm{H_p} \rightarrow 0.5\ \mathrm{N_2O} + \mathrm{Cyt_{552}} + 0.5\ \mathrm{H_2O} \tag{S.15}$$

R_ATP_synt [4]:

$$\mathrm{ADP} + \mathrm{Pi} + 3\ \mathrm{H_p} \rightarrow \mathrm{ATP} + \mathrm{H_2O} + 3\ \mathrm{H_c} \tag{S.16}$$

S2.4 Reaction network for NOB

R_biomass [4] (biomass coefficient $113\ \mathrm{g\ dW/mol}$):

$$\begin{aligned} &15\ \mathrm{ATP} + 12\ \mathrm{NADH} + 0.25\ \mathrm{protein} + 32\ \mathrm{maint} + 5\ \mathrm{CO_2} + 7\ \mathrm{H_c} \\ &\rightarrow 15\ \mathrm{ADP} + 10\ \mathrm{NAD} + 15\ \mathrm{Pi} + 4\ \mathrm{O_2} \end{aligned} \tag{S.17}$$

R_maint [4]:

$$\mathrm{ATP} + \mathrm{H_2O} \rightarrow \mathrm{ADP} + \mathrm{Pi} + \mathrm{H_c} + \mathrm{maint} \tag{S.18}$$

R_protein [4]:

$$8.9\ \mathrm{ATP} + 4\ \mathrm{NH_3.NH_4} \rightarrow 8.9\ \mathrm{ADP} + 8.9\ \mathrm{Pi} + 8.9\ \mathrm{H_c} + \mathrm{protein} \tag{S.19}$$

Jnrj8 [5]:

$$2\ \mathrm{Cytc_{550red}} + \mathrm{HNO_2.NO_2} + \mathrm{H_2O} \rightarrow 2\ \mathrm{Cytc_{550ox}} + 2\ \mathrm{H_c} + \mathrm{HNO3.NO3} \tag{S.20}$$

Jnrj9 [5]:

$$\mathrm{H_p} + \mathrm{Cytc_{550ox}} + \mathrm{HNO_2.NO_2} \rightarrow \mathrm{Cytc_{550red}} + \mathrm{H_2O} + \mathrm{NO} \tag{S.21}$$

Jnrj10 [5]:

$$4\ \mathrm{H_p} + \mathrm{UQ} + 2\ \mathrm{H_2O} + 2\ \mathrm{NO} \rightarrow \mathrm{UQH_2} + 4\ \mathrm{H_p} + 2\ \mathrm{HNO_2.NO_2} \tag{S.22}$$

Jnrj11 [5]:

$$\mathrm{Cytc_{550red}} + \mathrm{H_2O} + \mathrm{NO} \rightarrow \mathrm{Cytc_{550ox}} + \mathrm{H_c} + \mathrm{HNO_2.NO_2} \tag{S.23}$$

Jtermox_dissip [5] (dissipation (loss) of proton motive force (PMF) by proton diffusion):

$$2\ \mathrm{Cytc_{550ox}} + 4\ \mathrm{H_c} + 0.5\ \mathrm{O_2} + 1.12\ \mathrm{H_p} \rightarrow 2\ \mathrm{H_p} + 2\mathrm{Cytc_{550red}} + \mathrm{H_2O} + 1.12\ \mathrm{H_c} \tag{S.24}$$

JNAD [5]:

$$4\ \mathrm{H_p} + \mathrm{NAD} + \mathrm{UQH_2} \rightarrow \mathrm{UQ} + \mathrm{NADH} + 5\ \mathrm{H_c} \tag{S.25}$$

JATP [5]:

$$3\ \mathrm{H_p} + \mathrm{ADP} + \mathrm{Pi} \rightarrow \mathrm{ATP} + 3\ \mathrm{H_c} + \mathrm{H_2O} \tag{S.26}$$

R_nirBD [7] (nitrite reduction to ammonium, accounting for nitrogen assimilation, nitrite detoxification, and NAD regeneration):

$$\mathrm{HNO_2.NO_2} + 3\ \mathrm{NADH} + 4\ \mathrm{H_c} \rightarrow \mathrm{NH_3.NH_4} + 3\ \mathrm{NAD} + 2\ \mathrm{H_2O} \tag{S.27}$$

S2.5 Uptake kinetics

- Ammonium/ammonia ($NH_3.NH_4$) uptake rate limits are specified as a Monod function of NH_3:

$$\frac{[NH_3]}{\frac{1}{\alpha} + \frac{[NH_3]}{V}}, \tag{S.28}$$

where $V = 6.48 \times 10^{-13}$ mol/cell/day (maximum cell-specific uptake rate) and $\alpha = 2.49 \times 10^{-8}$ L/cell/day (affinity [1]) for the calibrated AOB model. Note that the model does not differentiate between ammonium and ammonia uptake, since in the bioreactor the two compounds are at dissociation equilibrium, determined by pH and the sum of ammonium and ammonia concentrations. Nevertheless, uptake kinetics were specified in terms of ammonia concentrations according to findings by Suzuki *et al.* [8] that suggest that ammonia is likely the limiting substrate.

Random AOB strains had modified kinetics:

$$\frac{[NH_3]}{\frac{1}{\alpha_r(1-\kappa_r)} + \frac{[NH_3]}{\kappa_r V_r}}, \tag{S.29}$$

where κ_r is chosen randomly from 0 to 1, V_r is chosen randomly from $V/10$ to $10V$, and α_r is chosen randomly from $\alpha/10$ and 10α. We randomly varied V and the affinity α (as opposed to the half-saturation concentration) according to Aksnes & Cao [1], who showed that affinity, rather than half-saturation concentration, is an inherent biological trait. The random parameter κ_r accounts for trait-offs between affinities and maximum cell-specific uptake rates, as suggested by [6].

- Nitrite/nitrous acid ($HNO_2.NO_2$) uptake rate limits are specified as a Monod function of $HNO_2.NO_2$:

$$\frac{[HNO_2.NO_2]}{\frac{1}{\alpha} + \frac{[HNO_2.NO_2]}{V}}, \tag{S.30}$$

where $V = 7.31 \times 10^{-13}$ mol/cell/day and $\alpha = 3.19 \times 10^{-9}$ L/cell/day for the calibrated AOB model. Note that the model does not differentiate between nitrite and nitrous acid uptake, since in the bioreactor the two compounds are at dissociation equilibrium determined by pH.

Random NOB strains had modified kinetics:

$$\frac{[HNO_2.NO_2]}{\frac{1}{\alpha_r(1-\kappa_r)} + \frac{[HNO_2.NO_2]}{\kappa_r V_r}}, \tag{S.31}$$

where κ_r is chosen randomly from 0 to 1, V_r is chosen randomly from $V/10$ to $10V$, and α_r is chosen randomly from $\alpha/10$ and 10α.

S2.6 Community-scale dynamics

The membrane bioreactor model keeps track of the cell concentrations of each AOB and NOB strain, as well as extracellular ammonia/ammonium ($\mathrm{NH_3}.\mathrm{NH_4}$), nitrite/nitrous acid ($\mathrm{HNO_2}.\mathrm{NO_2}$) and nitrate/nitric acid ($\mathrm{HNO_3}.\mathrm{NO_3}$) concentrations over time. The bioreactor is assumed to be well mixed and well oxygenated. Let $N_i(t)$ be the cell concentration for strain i (AOB or NOB), $C_j(t)$ the concentration of metabolite j and $E_{ij}(t)$ the net export rate of metabolite j by each cell of strain i, at time t. Note that $E_{ij}(t)$ is calculated by solving a linear FBA problem for each strain and at each time step. The constraints of the FBA problems, and thus their solutions, depend on the maximum substrate uptake rates, which are given by Monod kinetics as described above. All population sizes N_i are described by ordinary differential equations (ODEs) of the following form:

$$\frac{dN_i(t)}{dt} = \frac{1}{m_i} B_i(t) N_i(t) - \lambda_i N_i(t). \tag{S.32}$$

Here, λ_i is the exponential death rate of strain i, i.e. the inverse of its expected life time, $B_i(t)$ is the per-cell biosynthesis rate determined by FBA and m_i is the cell mass. Similarly, all metabolite concentrations C_i are described by ODEs of the following form:

$$\frac{dC_j}{dt} = r \cdot \left[\tilde{C}_j - C_j(t)\right] + \sum_i E_{ij}(t) N_i(t). \tag{S.33}$$

Here, r is the hydraulic turnover rate (feed rate over bioreactor volume) and $\tilde{C}_j$ is the concentration of the metabolite in the feed. The last term is a sum over all cell populations, accounting for microbial production or consumption of the metabolite.

References

[1] Aksnes DL, Cao FJ (2011) Inherent and apparent traits in microbial nutrient uptake. *Marine Ecology Progress Series* 440: 41–51

[2] Clegg SL, Whitfield M (1995) A chemical model of seawater including dissolved ammonia and the stoichiometric dissociation constant of ammonia in estuarine water and seawater from- 2 to 40 C. *Geochimica et Cosmochimica Acta* 59: 2403–2421

[3] de Boer W, Laanbroek H (1989) Ureolytic nitrification at low pH by *Nitrosospira* spec. *Archives of Microbiology* 152: 178–181

[4] Perez-Garcia O, Villas-Boas SG, Swift S, Chandran K, Singhal N (2014) Clarifying the regulation of $\mathrm{NO}/\mathrm{N_2O}$ production in *Nitrosomonas europaea* during anoxic–oxic transition via flux balance analysis of a metabolic network model. *Water Research* 60: 267–277

[5] Poughon L, Dussap CG, Gros JB (2001) Energy model and metabolic flux analysis for autotrophic nitrifiers. *Biotechnology and Bioengineering* 72: 416–433

[6] Smith SL, Yamanaka Y, Pahlow M, Oschlies A (2009) Optimal uptake kinetics: physiological acclimation explains the pattern of nitrate uptake by phytoplankton in the ocean. *Marine Ecology Progress Series* 384: 1–12

[7] Starkenburg SR, Chain PSG, Sayavedra-Soto LA, Hauser L, Land ML, Larimer FW, Malfatti SA, Klotz MG, Bottomley PJ, Arp DJ, Hickey WJ (2006) Genome sequence of the chemolithoautotrophic nitrite-oxidizing bacterium *Nitrobacter winogradskyi* Nb-255. *Applied and Environmental Microbiology* 72: 2050–2063

[8] Suzuki I, Dular U, Kwok SC (1974) Ammonia or ammonium ion as substrate for oxidation by *Nitrosomonas europaea* cells and extracts. *Journal of Bacteriology* 120: 556–558

[9] Wittebolle L, Vervaeren H, Verstraete W, Boon N (2008) Quantifying community dynamics of nitrifiers in functionally stable reactors. *Applied and Environmental Microbiology* 74: 286–293